JOURNAL OF MATERIALS SCIENCE 17 (1982) 2227–2238

Dislocation etch pit formation on non-metallic crystals

K. SANGWAL
Institute of Physics, Technical University of Łódź, Wólczańska 219, 93-005 Łódź, Poland

Experimental results available in the literature on selective etch pit formation on non-metallic crystals (excluding semiconductors) are discussed against the background of thermodynamic and topochemical adsorption theories of etching. The main purpose of the article is to deduce general principles involved in the formation of dislocation etch pits, and to better define the role of addition of salts to a solvent, of reaction products and solvents in etch pit formation. In addition, attention is focussed on the need for experimental determination of the absolute values of the parameters involved in thermodynamic theories in order to explain the results quantitatively.

1. Introduction

Dislocation etchants for a variety of crystals are at present discussed in the literature. At the same time different types of theories of dissolution exist. It is therefore opportune to review the experimental data on etch pit formation in the light of the theories. The present paper is an attempt in this direction where only non-metallic crystals are considered. Metals and semiconductors are not included, because their dissolution mechanism involved complex processes of electrochemistry. The main aim of this article is to deduce some general principles involved in the formation of dislocation etch pits, to better define the role of additive salts to a solvent, of reaction products and solvents during etch pit formation, and to point out the urgency for experimental determination of the absolute values of the parameters involved in the thermodynamic theories.

2. Resumé of the theories

Among the different types of existing theories of dissolution, thermodynamic and topochemical adsorption theories are of particular interest because they deal with the formation of dislocation etch pits on a crystal surface.

A comprehensive account of the different types of theories is given by Heimann [1].

2.1. Topochemical adsorption theories

These theories essentially express the dissolution rate in terms of chemical reactions on the crystal surface [1, 2]. It is considered [2] that etch pits at the sites of dislocations are formed as a consequence of enhanced dissolution caused by the preferred adsorption of a reactant at that site because of the strain associated with the dislocation. Reactants that adsorb more strongly produce better contrasting pits.

Topochemical theories are particularly attractive for crystalline substances, the dissolution of which involves the formation of reaction products, but they have their own limitations. One serious limitation stems from the fact that each etching system has to be treated independently. Furthermore, details of the adsorption processes are far from being clear.

2.2. Thermodynamic theories

The thermodynamic theories are based on the postulate that the energy localized in the vicinity of a dislocation lowers the free energy required for the nucleation of a cavity of unit depth in the surface at the site of the dislocation. This decrease in the free energy is the cause of preferred dissolution of the surface at the emergence points of dislocations. The free energy change associated with the formation of a mono-molecular pit at

0022–2461/82/082227–12$03.94/0

the dislocation site, ΔG, is given by

$$\Delta G = 2\pi r a\gamma - \frac{\pi r^2 a\Delta\mu}{\Omega} - aE_d \quad (1)$$

where r is the radius of the cavity, a is its height, $\Delta\mu$ the change in free energy during dissolution (chemical potential), Ω the molecular volume of the crystal, and γ the specific surface free energy of an atom or molecule going from the solid surface into the solution. The chemical potential is given by

$$\Delta\mu = -kT\ln(c/c_0), \quad (2)$$

where c_0 is the saturation concentration of the material in an etching medium and c is the actual concentration at the dislocation site.

The localized energy per unit length at a dislocation, E_d, is expressed by

$$E_d = A\ln(r_1/r_0), \quad (3a)$$

$$E_d = \frac{\alpha G b^2}{4\pi}(r_1/r_0) \quad (3b)$$

in Cabrera's and Schaarwächter's theories, respectively. Here Equation 3a represents the elastic strain energy and Equation 3b the dislocation core energy, $A = Gb^2/4\pi(1-\mu)$ for edge dislocations and $A = Gb^2/4\pi$ for screw dislocations (where G is the shear modulus, b is the modulus of the Burgers vector of the dislocation and μ the Poisson's ratio), r_0 is the radius of the dislocation core beyond which elasticity theory holds, r_1 is the outer radius of the strained region of the crystal, and α is a constant equal to about 1.5 or 2 for screw or edge dislocations, respectively.

In the Cabrera's theory [3, 4] the free energy change involved in the formation of a dislocation pit, ΔG_n^*, is given by

$$\Delta G_n^* = \Delta G_s^*(1-\xi)^{1/2}, \quad (4)$$

where the maximum free energy change associated with the formation of a unit pit in a perfect surface is expressed by

$$\Delta G_s^* = \frac{\pi\gamma^2 a\Omega}{\Delta\mu}, \quad (5)$$

and

$$\xi = \frac{2A\Delta\mu}{\pi\Omega\gamma^2}. \quad (6)$$

The potential necessary for the nucleation of an etch pit is obtained when $\xi \to 1$, i.e.

$$\Delta\mu = -kT\ln(c/c_0) < \frac{2\pi^2\gamma^2\Omega}{Gb^2}. \quad (7)$$

From Equations 4, 6 and 7 it may be inferred that larger $\Delta\mu$ and b and smaller γ are favourable for etch pit formation at a dislocation site.

According to Cabrera [5] the slope of a dislocation etch pit, $m = a/R$, is related to the material concentration, $c(R)$, at a distance, R, from the dislocation site, the concentration, $c(0)$, at the dislocation source and the concentration, c', away from the dislocation site in the solvent, by the relationship

$$\frac{c(0)-c'}{c(R)-c'} = \frac{\pi}{\ln(1/m)} < 1. \quad (8)$$

In particular when $c' \to 0$, denoting $c(0)$ by c and $c(R)$ by c_0 the pit slope may be given as

$$m = \frac{a}{R} = \exp(\pi c_0/c) = \exp\left[\pi\exp\left(\frac{\Delta\mu}{kT}\right)\right]. \quad (9)$$

Thus pit slope is a function of $\Delta\mu$. In the case of poisoning of dissolution ledges the radius of curvature of the pit, R, is reduced and hence pits become visible. This implies that the role of the impurity is to increase c_0/c. Cabrera [5] suggests that an impurity cannot slow down the ledge motion and decrease γ simultaneously.

In the Schaarwächter theory [6] the maximum free energy change is

$$\Delta G_n^* = p\Delta G_s^*, \quad (10)$$

where

$$p = \left(\frac{1-\alpha qGb}{4\pi\gamma}\right)^2, \quad (11)$$

with the value of the constant $q \simeq 0.1$. Since the value of G/γ^2 for the same plane of similar type of crystals is essentially constant†, it may be seen

†The relationships between yield strength, σ_y, bulk modulus, K, shear modulus, G, and Vickers hardness, H_v, are [7, 8]:

$$\sigma_y = \sqrt{3}K,$$
$$H_v = 3\sigma_y,$$
$$K = \frac{2G(1+\mu)}{3(1-2\mu)}.$$

For a value of Poisson's ratio $\mu \simeq 0.3$, $H_v = 11.2G$. Since H_v/γ^2 is constant [9], we have G/γ^2 = constant. The ratio of H_v/G from experimental values of H_v is about 0.1, but the absolute value is not of concern here.

that the value of p decreases with an increase in the hardness of the crystals.

The rates of dissolution along the dislocation line, v_n, and along the surface, v_t, are given by [10]

$$v_n = a\nu \exp[-(\Delta G_n^* + \Delta H)/kT], \quad (12)$$

$$v_t = \alpha x_s \beta \nu \exp[-\Delta H/kT], \quad (13)$$

where x_s is the mean displacement of an atom diffusing from a kink site to an adsorbed position, $\beta \leqslant 1$ is a factor which accounts for the hindrance of the motion of ledges in the presence of an impurity, $\sigma = 1 - c/c_0$ the undersaturation, and ΔH the free energy change for a molecule going from crystal surface into solution, and ν is the frequency factor. Substituting the values of ΔG_s^* and taking $k^* = \beta x_s/a$ (defined as ledge mobility factor), for large undersaturations the pit slope may be written from Equations 12 and 13 as

$$m = \frac{v_n}{v_t} = \frac{1}{k^* \exp(\pi p a \Omega \gamma^2 / \Delta\mu kT).} \quad (14)$$

In contrast with the Cabrera's treatment, here no potential barrier exists for etch pit nucleation. The ability of observing a pit depends on the instrument used. In Equation 14 there are 4 parameters, viz. k^*, $\Delta\mu$, γ and p, which determine the pit slope. Smaller values of k^*, p and γ and a large $\Delta\mu$ lead to the formation of contrasting pits. Cabrera's treatment also yields similar conclusions but Schaarwächter's theory connects the dependence of pit slope on different parameters more explicity.

3. Summary of etching behaviour

The typical compositions of dislocation etchants for various crystals together with their solubility in water and the values of the specific free energy of the crystals in vacuum, γ_{vac}, G and lattice data are listed in Table I.

Investigations of the etching behaviour of water-soluble crystals have shown [33, 39–41, 44, 45, 56–58] that water easily forms etch pits on these crystals. The etching capability decreases along the series of homologous alcohols and acids with the addition of a–CH_2 group [24, 40, 41, 56]. This behaviour is shown in Figs 1 and 2 for potassium dihydrogen phosphate (KDP) crystals. It is obvious that with a change in the solvent not only the etching capability changes but the pit morphology changes, and that different surfaces behave differently to the same series of solvents.

4. Discussion

4.1. Crystal structure

Etch pits are easily formed by a solvent on those water-soluble crystals which have large lattice constants. Compare, for example, the etching behaviour of borax, sucrose, alums etc., with that of alkali halides.

The Burgers vector, **b**, of a dislocation is intimately connected with the lattice parameters (Table II). Crystals possessing lower symmetry have larger Burgers vectors and it is these very crystals on which etch pits are easily formed. That the Burgers vector plays a vital role in etch pit formation has been well established in the case of CsI crystals [60]. In terms of Equation 14 this observation is associated with a decrease in p (Equation 11).

4.2. Solvent effects

There is no correlation between etch pit formation in a solvent and the solubility of the crystals. Water forms etch pits on sparingly soluble crystals such as BaF_2 and $CaSO_4 \cdot 2H_2O$ as well as on highly soluble crystals such as borax, alums, KDP, and $K_2Cr_2O_7$. This inference is contrary to the common belief [27, 61, 62] that in order to etch a crystal surface selectively a solvent in which the crystal is slightly soluble should be selected. It is of course true that the time of etching for poorly soluble crystals is excessively long while on fairly soluble crystals pits are formed within seconds. The etching time in the case of the former crystals can be decreased by the addition of a reactant (e.g. acid) while for the latter type of crystals etching time may be increased by the addition of an organic solvent (for example an alcohol or a ketone) of low dielectric constant in which the crystal is less soluble.

For a given crystal where γ and p are constant, the pit slope, according to Equation 14, can increase either by a decrease in k^* or an increase in $\Delta\mu$, the latter through an increase in crystal solubility. Alternatively, solvents in which a crystal is less soluble can yield poorly contrasting etch pits by an increase in k^* or a decrease in $\Delta\mu$.

Crystals having large γ and G (i.e. hard crystals) as a rule are poorly soluble in water and consequently correspond to systems with smaller $\Delta\mu$. The situation is analogous to that of the etching of water-soluble crystals in organic solvents discussed above. According to Equation 14 the pit

TABLE I Composition of some typical selective etchants for non-metallic crystals and their lattive parameters, solubility c_0, shear modulus, G, and surface free energy in vacuum γ_{vac}

Crystal lattice	Crystal name	Lattice data (nm)	Solubility, c_0 (g per 100 ml H_2O)	G [15] (10^{-10} N m^{-2})	γ_{vac}* (10^{-3} J m^{-2})	Selective etchants		
						Etchant	Plane investigated	Ref.
Cubic	LiF	$a = 0.40262$	0.27 (18) [11]	6.35	340 [16]	HCOOH	(100), (111)	[22]
						$H_2O + FeCl_3$	(100)	[23]
	NaCl	$a = 0.5627$	35.86 [11]	1.28	130 [16]	CH_3OH, HCOOH	(100), (110) (111)	[24]
	KCl	$a = 0.6293$	34.4 (20) [11]	0.63	107 [17]	C_2H_5OH + $Pb(CH_3CO_2)_2$	(100)	[25]
	KBr	$a = 0.6586$	65.2 (20) [11]	0.51	92 [17]	C_2H_5OH	(100)	[26]
						CH_3COOH	(100)	[27]
	KI	$a = 0.7052$	144.5 (20) [11]	0.37	75 [17]	C_3H_7OH	(100)	[27]
	RbI	$a = 0.7325$	169 (25) [11]	0.28	–	Hr. Alc. + salt	(100)	[28]
	CsI	$a = 0.4562$	85.6 (25) [11]	0.63	–	Alc. + Cu^{2+}	(100)	[29]
	$NaClO_3$	$a = 0.6570$	95.9 (20) [11]	–	–	HCOOH, CH_3COOH	(100), (110) (111)	[30]
	$NaBrO_3$	$a = 0.6705$	36.4 (20) [11]	–	–	H_2O	(111)	[31]
	$Sr(NO_3)_2$	$a = 0.7763$	70.4 (20) [11]	1.58	–	HCOOH	(100), (110), (111)	[32]
	$KAl(SO_4)_2 \cdot 12H_2O$	$a = 1.2130$	11.4 (20) [12]	0.85	237 [13]	H_2O	(111)	[33]
	$KCr(SO_4)_2 \cdot 12H_2O$	$a = 1.2197$	24.39 (25) [12]	0.75	–	H_2O	(111)	–
	MgO	$a = 0.42117$	0.0086 (30) [12]	15.5	1200 [16]	Dil. and conc. acids	(100), (110), (111)	[34]
	BaF_2	$a = 0.6196$	0.161 (20) [11]	2.53	280 [16]	acids	(111)	[35, 36]
	CaF_2	$a = 0.5462$	0.0016 (18) [12]	3.39	450 [16] 433 [18]	acids	(111)	[37, 38]
Tetragonal	$NH_4H_2PO_4$ (ADP)	$a = 0.751$ $c = 0.753$	36.5 (20) [13]	0.86	265 [19]	H_2O	{101}	[39]
	KH_2PO_4 (KDP)	$a = 0.743$ $c = 0.694$	22.6 (20) [13]	1.26	385 [19]	H_2O	{101}	[39]
	RbH_2PO_4	$a = 0.7607$ $c = 0.7302$	42 (20) [14]	1.06	283 [19]	50% CH_3COOH + salt	{100}	[19]
	$NiSO_4 \cdot 6H_2O$	$a = 0.68$ $c = 1.83$	38.4 (20) [11]	1.16	–	C_2H_5OH	(010)	[42]
Orthorhombic	$MgSO_4 \cdot 7H_2O$	$a = 1.1940$ $b = 1.2030$ $c = 0.6870$	35.5 (20) [13]	0.78	153–214 [18]	H_2O	Various planes	–

TABLE I (*continued*)

Crystal lattice	Crystal name	Lattice data (nm)	Solubility, c_0 (g per 100 ml H_2O)	G [15] (10^{-10} N m^{-2})	γ_{vac}* (10^{-3} J m^{-2})	Selective etchants		
						Etchant	Plane investigated	Ref.
	$KClO_4$	$a = 0.8834$ $b = 0.5650$ $c = 0.7240$	1.67 (20) [11]	–	105 [20]	H_2SO_4 + dil aq · $4Na_2SO_3$	(001), (210)	[43]
	$KHC_4H_4O_6$	$a = 0.7609$ $b = 1.0652$ $c = 0.7762$	0.53 (20) [13]	–	–	H_2O, HCOOH	(010)	[44]
	$KNaC_4H_4O_6 \cdot 4H_2O$	$a = 1.1867$ $b = 1.4236$ $c = 0.6213$	39.84 (20) [11]	1.19	–	H_2O	(001)	[45]
	$CaC_4H_4O_6 \cdot 4H_2O$	$a = 0.924$ $b = 1.063$ $c = 0.966$	0.036 (25) [11]	–	182 [21]	H_2O, HCOOH, CH_3COOH	(1 1 0)	[46]
	$SrC_4H_4O_6 \cdot 4H_2O$	$a = 0.948$ $b = 1.096$ $c = 0.946$	0.1765 (25) [11]	–	151 [21]	H_2O, HCOOH CH_3COOH Aq.NH_4Cl	(110) (110)	[46] [47]
	α-Ca $(HCO_2)_2$	$a = 1.0163$ $b = 1.3381$ $c = 0.6271$	16.6 (20) [11]	–	–	H_2O, HCOOH	Various planes	–
Trigonal	$NaNO_3$	$a = 0.6320$ $\alpha = 47°14$	87.6 (20) [11]	1.16	101 – 153 [18]	CH_3COOH	(100)	[48]
	$C(NH_2)_3Al(SO_4)_2 \cdot 6H_2O$ (GASH)	$a = 1.1737$ $c = 0.8948$	67.5 (20) [11]	0.92	–	H_2O	(0001)	[49]
Monoclinic	$CaSO_4 \cdot 2H_2O$	$a = 0.628$ $b = 1.515$ $c = 0.659$ $\beta = 127°31$	0.206 (20) [11]	0.86	153 [18]	H_2O Dil. HNO_3	(010) (010)	[50] [51]
	$K_2C_4H_4O_6 \cdot \frac{1}{2} H_2O$	$a = 1.5490$ $b = 0.5049$ $c = 2.0101$ $\beta = 90°51$	155 (20) [11]	0.9	–	C_2H_5OH + glycerine	(001), (100)	[52]
	$NaB_4O_7 \cdot 10H_2O$ (Borax)	$a = 1.182$ $b = 1.061$ $c = 1.230$ $\beta = 106°31$	2.5 (20) [11]	–	153 214 [18]	H_2O + acetone	Various planes	[53]
	TGS	$a = 0.9417$ $b = 1.2643$ $c = 0.5735$ $\beta = 110°23$	27 (20) [13]	1.0	–	H_2O	(010), (100)	[54]

	$C_{12}H_{22}O_{11}$ sucrose	$a = 1.086$ $b = 0.872$ $c = 0.775$ $\beta = 103°$	204 (20) [13]	–	260 [13]	50 % C_2H_5OH	{100}	[55]
Triclinic	$K_2Cr_2O_7$	$a = 0.734$ $b = 0.749$ $c = 1.339$ $\alpha = 96°20$ $\beta = 97°56$ $\gamma = 90°30$	12.48 (20) [11]	–	–	H_2O, alc., org. acids	Various planes	[56]
	$CuSO_4 \cdot 5H_2O$	$a = 0.612$ $b = 1.070$ $c = 0.597$ $\alpha = 82°16$ $\beta = 107°26$ $\gamma = 102°40$	25.5 (20) [11]	–	214 [18]	H_2O	Various planes	–
Hexagonal	CdI_2	$a = 0.424$ $c = 0.684$	84.8 (20) [11]	0.55	–	H_2O	(0001)	[57]
	$\alpha - LiIO_3$	$a = 0.5481$ $b = 0.5172$	125 (15) [12]	–	–	H_2O	$(000\bar{1})$	[58]

*In [13, 18–21] Mohs and Vickers hardness are available. The conversion of hardness into surface energy is given in [9]..
†Temperature in parenthesis (° C).

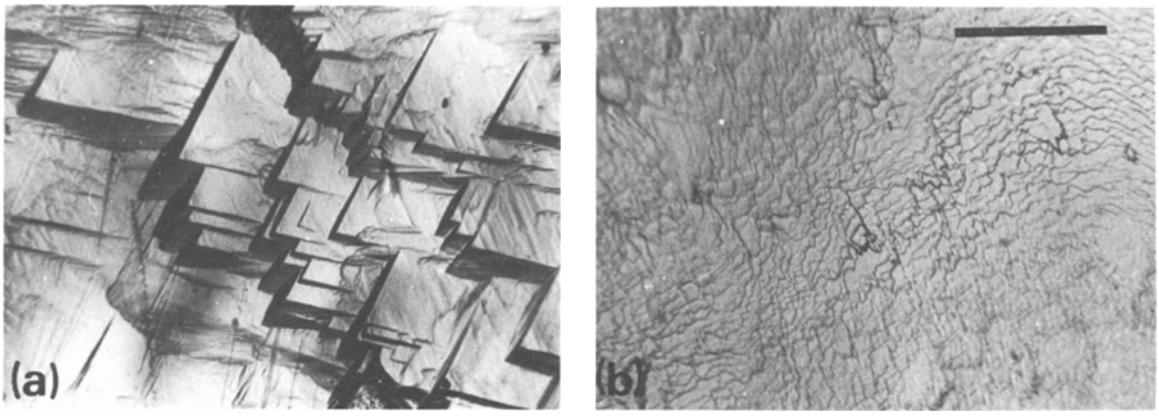

Figure 1 Etch patterns produced on the {1 0 1} surface of KDP by (a) H_2O and (b) CH_3OH after a 2 sec and 4 h etching, respectively. Note the absence of pits in (b). The marker indicates 0.3 mm.

slope is small in this case. In fact it is common knowledge that it is difficult to etch hard crystals. In order to produce contrasting dislocation etch pits on the surfaces of hard crystals it is therefore necessary to use a reagent in which these crystals are more soluble.

Different solvents lower the surface free energy of a crystal to a different extent. Solvents which lead to a relatively greater decrease in γ are, according to Equation 14, expected to produce better contrasting etch pits.

The changes in γ are the consequence of adsorption of a solvent on the crystal surface. In the case of non-polar solvents the energy of adsorption increases as the number of groups constituting the solvent molecule increases [63]. Consequently, the lowering in γ by such solvents increases with an increase in the number of groups constituting the molecule. Hence solvents which decrease γ are expected to produce contrasting pits. The formation of etch pits on MgO, BaF_2, CaF_2, etc., appears to be due to such a process. However, it should be remembered that a change in γ is also accompanied by changes in $\Delta\mu$, k^* and p. Therefore the resulting pit slope is determined by the combined effect of all these changes.

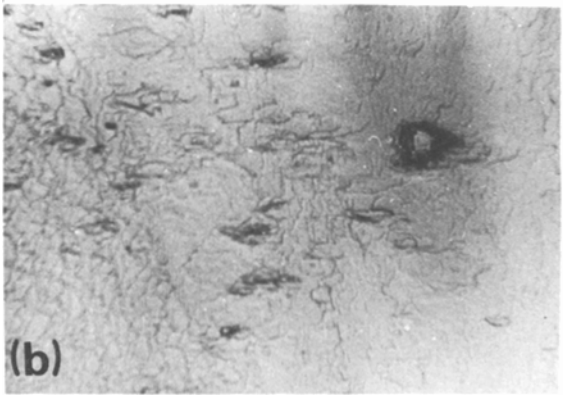

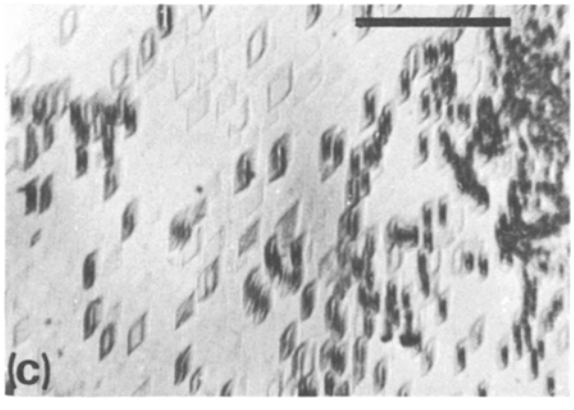

Figure 2 Etch pits produced on the (0 1 0) surface of KDP by (a) H_2O, (b) CH_3OH and (c) CH_3COOH after etching for 2 sec, 4 h and 6 min, respectively. Shallow pits may be seen in (b). The marker indicates 0.3 mm.

TABLE II Magnitude and direction of Burgers vector of glide dislocations in various crystals*

Lattice	Magnitude of Burgers vector	Direction of Burgers vector
Simple cubic	a	$\langle 100 \rangle$
Body centred cubic	$\sqrt{3}a/2, a$	$\frac{1}{2}\langle 111 \rangle, \langle 100 \rangle$
Face centred cubic	a	$\langle 110 \rangle$
CsCl-type	$a, \sqrt{2}a$	$\langle 001 \rangle, \langle 110 \rangle$
NaCl-type	$a/\sqrt{2}$	$\frac{1}{2}\langle 110 \rangle$
CaF_2	a	$\langle 001 \rangle$
Simple tetragonal	a, c	$\langle 100 \rangle, \langle 001 \rangle$
Face-centred tetragonal ($c/a < \sqrt{2}$)	$(a^2/2 + c^2/2)^{1/2}, a, c$	$\frac{1}{2}\langle 111 \rangle, \langle 100 \rangle, \langle 001 \rangle$
Face-centred tetragonal ($c/a > \sqrt{2}$)	$(a^2/2 + c^2/2)^{1/2}, a$	$\frac{1}{2}\langle 111 \rangle, \langle 100 \rangle$
Rhombohedral ($\alpha < 90°$)	$a, 2a \sin \alpha/2,$ $a(1 + 4 \sin^2 \alpha/2)^{1/2}$	$\langle 100 \rangle, \langle 1\bar{1}0 \rangle, \langle 1\bar{1}1 \rangle$
Rhombohedral ($\alpha > 90°$)	$a, 2a \cos \alpha/2,$ $3a(1 - (\frac{4}{3}) \sin^2 \alpha/2)^{1/2}$	$\langle 100 \rangle, \langle 110 \rangle, \langle 111 \rangle$
Hexagonal	a, c	$\frac{1}{3}\langle 11\bar{2}0 \rangle, \langle 0001 \rangle$

*Except for CsCl-, NaCl- and CaF_2-type crystals, the values are taken from [59].

Once the adsorption effects are accepted as the cause of pit formation at dislocations, it is obvious that a solvent can also lead to changes in the mobility of dissolution ledges emanating from the dislocation site. This effect in essence is similar to the effect of an inhibitive impurity added to a solvent used for the selective etching of alkali halides (see Section 4.4). However, adsorption effects by solvents in slowing down the mobility of dissolution ledges are expected to be poor for reasons which we will consider in Sections 4.4 and 4.5.

4.3. Surface orientation

Dislocation etch pits are formed on all surface orientations of water-soluble crystals by solvents in which a crystal is more soluble. Examples illustrating this feature are NaCl [24] KDP [41] and $K_2Cr_2O_7$ [56]. It has also been reported that the revelation of selective etch pits is difficult on certain surfaces (e.g. the $\{110\}$ face of NaCl [24] and the $\{101\}$ surface of KDP [41]) by solutions in which a crystal is poorly soluble.

In the case of sparingly-soluble crystals for which chemically active reagents (e.g. acids for MgO [64]) are the etchants, the reverse effect is noted. In such crystals etch pits are easily produced on surfaces which are difficult to etch selectively in the case of soluble crystals.

The theoretical surface free energy of halide-type crystals in vacuum varies in the sequence $\{111\} > \{110\} > \{100\}$ [17]. If the same order were maintained in aqeuous solutions, then, according to Equation 5 it should be difficult to produce pits on $\{111\}$ surfaces. From the experimental data on hardness of the above mentioned surfaces [65], on the other hand, one finds the surface energy to be independent of surface orientation (cf [9]). Assuming again that γ decreases equally for all surfaces we find that all these faces should reveal etch pits to the same extent.

Baranova and Nadgornyi [24] found that the polishing rates of $\{111\}$, $\{110\}$ and $\{100\}$ surfaces of NaCl crystals are practically the same in a solvent. Identifying the polishing rate with $\Delta\mu$, it follows from Equation 14 that etch pits should be revealed equally on all the surfaces. Sangwal *et al.* [64] reported that the polishing rate is the lowest for the $\{110\}$ face. This implies that pit slope should be small i.e. polishing should take place. Obviously these expectations are in disagreement with the experimental observations, and precise data on γ and k^* are required to understand the surface orientation effects.

4.4. Effect of additive impurities

It is well known that in order to reveal etch pits on the $\{100\}$ face of alkali halides, it is often necessary to add an inorganic salt to the solvent. Gilman *et al.* [23] observed that in LiF the addition of an impurity reduces the lateral growth of etch pits while the etch rate along the dislocation line practically remains the same. Baranova and Nadgornyi [66] found that in the case of NaCl an additive can behave

both ways, it can increase or decrease both v_t and v_n simultaneously. One obvious effect of the additive therefore is to alter the value of k^* and hence, according to Equation 14, a change in pit slope. An increase in v_t implies an increase in k^* and therefore a decrease in pit slope. In this case, however, the contrast is maintained (or increased) by virtue of an increase in v_n caused by a decrease in ΔG_n^* (through an increase in $\Delta\mu$ and a decrease in γ; cf Equations 10 and 11).

Gilman *et al.* [23] found that visible etch pits are produced on {100} plane of LiF at $c/c_0 \leqslant 0.25$, while Kostin and his co-workers [67] observed etch pits on the cube planes of NaCl even for c/c_0 values approaching unity. In the absence of sufficient data on c/c_0 values in the presence of different concentrations of an impurity used for the selective etching of crystals, a generalization about the role of additive in altering $\Delta\mu$ cannot be made. Also pertinent data on γ are needed to assess its role in etch pit formation.

It is known [23, 25, 27–29, 61, 62, 67] that additives that behave as inhibitors are generally sparingly or poorly soluble. These impurities can slow down the motion of dissolution ledges by virtue of their insoluble character [5]. It is also known (see e.g. [68, 69]) that inorganic salts in solutions exist in the form of complexes whose chemical constitution depends on the concentration of the salt in solution as well as on the concentration of another substance having an anion common with the additive salt. The instability constants of a series of complexes of a salt, in general, regularly decrease, i.e. each successive complex is more stable [70]. The enhanced nucleation rate along the dislocation line (due to the presence of the localized energy) and the lateral growth of pits may thus depend on the formation of successive complexes as a result of the availability of the common (or chemically similarly-behaving) ions. Denoting the additive impurity by MX_n and the alkali halide by AX, we may write the formation of successive complexes on the crystal surface at the dissolution site by the reaction:

$$[M(H_2O)_6]^{n+} + mAX \rightarrow [M(H_2O)_5X]^{(n-1)+} + (m-1)AX + A^+. \quad (15)$$

Assuming that the adsorption potential at the site of a dislocation (D), kink (K), ledge (L) and surface (S) changes in the sequence D > K > L > S (cf Section 2.1), we find that the substitution reaction is the fastest (Equation 15) at the dislocation site. Hence dissolution is more along the dislocation line. This type of mechanism explains not only the change in the lateral growth of pits but also the change in pit morphology.

A plot of instability constant of successive Fe(III) and Cu(II) complexes as a function of salt concentration [71] is illustrated in Fig. 3. The variation in pit slope observed on the {100} surface of LiF with the impurity concentration [72] is also shown in the figure. It may be noted that, except for the direction of their change, the two dependences are similar.

4.5. Effect of reaction products

The mechanism of etch pit formation on water-insoluble crystals by etchants that yield reaction products differs from that in the case of alkali halides by solvents containing additive impurities. In this case the reactant is responsible for pit

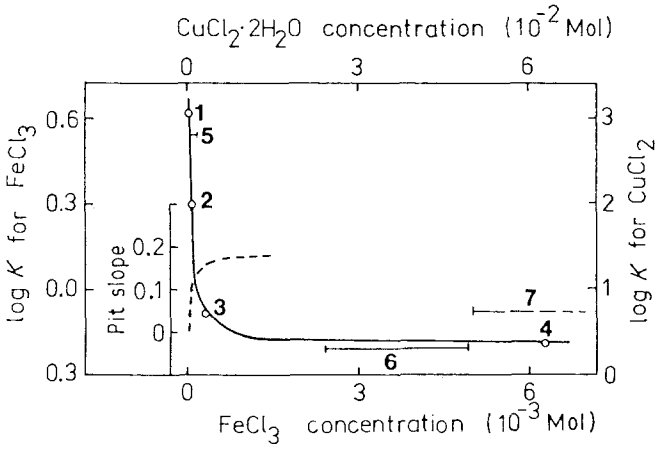

Figure 3 Graph illustrating the relationship between instability constant, K, for Fe(III) and Cu(II) complexes and the concentration of $FeCl_3$ and $CuCl_2 \cdot 2H_2O$ in water. 1, $[Fe(H_2O)_6]^{3+}$; 2, $[Fe(H_2O)_5Cl]^{2+}$; 3, $[Fe(H_2O)_4Cl_2]^+$; 4, $[FeCl_4]^-$; 5, $[Cu(H_2O)_6]^{2+}$; 6, $[Cu(H_2O)_5Cl]^+$ and 7, $[CuCl_4]^{2-}$. The dependence of pit slope on Fe^{3+} ion concentration in the case of etching of the (100) face of LiF [72] is shown by the dashed curve.

nucleation but the reaction product inhibits the motion of dissolution ledges. Since the etchants for water-insoluble crystals are invariably aqueous solutions, it is logical to assume that the reaction product does not exist as a compound (e.g. $MgCl_2$ during the dissolution of MgO in HCl) but exists in the form of aquo complex, the chemical constitution of which are dependent on the reactant concentration (cf [68, 69]). At low reactant concentrations when the aquo complex is unable to go over to the next stable form, inhibition may be expected to be the maximum. At high reactant concentrations when the complex is already stable, poor inhibition would take place. The main reason for such behaviour of a complex results from the fact that the crystal itself is practically "inert" so far as the formation of succeeding complexes is concerned (Equation 15).

The behaviour of a reaction product in causing the inhibiting action, discussed above, implies that at low reactant concentrations k^* is reduced. Thus although $\Delta\mu$ at low concentrations is low, constrasting pits are possible through a decreased k^*. At high concentrations when k^* is large contrasting pits again result because of an enhanced $\Delta\mu$ (Equation 14).

5. Conclusions

Conclusions can be drawn as follows.

(1) A solvent favourably produces etch pits at the sites of dislocations with large Burgers vectors.

(2) Selective etch pits are rapidly produced on water-soluble crystals by solvents, such as water, in which a crystal is more soluble. The time of etching for these crystals can be increased by the addition of an organic solvent of low dielectric constant in which a crystal is sparingly soluble. For water-insoluble crystals which are usually hard and in which dislocations are sluggishly revealed by water, the time of etching can be reduced by the addition of a reactant in which the crystal is more soluble. Solvents in which a crystal is more soluble are, in general, universal dislocation etchants and do not exhibit the orientation anisotropy of etch pit formation.

(3) The role of an additive poison in the case of alkali halides is quite complex. An inhibitor renders dislocation etch pit nucleation favourable and changes the motion of dissolution ledges by adsorbing at the newly creating surface as well as at the ledges spreading away from the ledge-generating source. It appears that etch pit slope is connected with the instability constant of the metal complex existing in an etchant. In the case of water-insoluble crystals which give reaction products, the contrasting nature of etch pits can be explained by considering that the adsorption of a reactant at the dislocation site is responsible for pit nucleation and that the reaction product (existing in the form of complexes) inhibits the motion of dissolution ledges.

It should be pointed out that although the formation of contrasting dislocation etch pits in different crystals can be explained along the above lines, there is as yet no direct experimental evidence to support this mechanism.

(4) The effect of Burgers vector of a dislocation, lattice constant, crystal solubility, additive concentration in a solvent, and reactant concentration on the formation of etch pits can qualitatively be understood in the light of the Schaarwächter theory of etch pit formation. However, in order to explain the results quantitatively, experimental determination of the absolute values of the parameters involved in the theory is necessary.

Acknowledgements

The author expresses his indebtedness to Mr M. Szurgot for his assistance with the compilation of the composition of etchants listed in Table I. This work was in part financed by the Polish Academy of Sciences under Research Project No. 06.7.3.

References

1. R. B. HEIMANN, "Auflösung von Kristallen" (Springer-Verlag, Wien, New York, 1975); Russian translation: "Rastvorenie Kristallov" (Nedra, Leningrad, 1979).
2. K. SANGWAL, *J. Mater. Sci.* **15** (1980) 237.
3. N. CABRERA, *J. Chim. Phys.* **53** (1956) 675.
4. N. CABRERA and M. M. LEVINE, *Phil. Mag.* **1** (1956) 450.
5. N. CABRERA, in: "The Surface Chemistry of Metals and Semiconductors" edited by H. C. Gatos, (John Wiley and sons, New York, Chichester, 1960) p. 71.
6. W. SCHAARWÄCHTER, *Phys. Status Solidi* **12** (1965) 375.
7. C. ZWIKKER, "Physical Properties of Solid Materials" (Pergamon Press, London, New York, 1955) Chaps 6 and 8.
8. O. H. WYATT and D. DEW-HUGHES, "Metals, Ceramics and Polymers" (Cambridge University Press, London, 1974) Chaps 5 and 6.
9. K. SANGWAL, *Cryst. Res. Technol.* **17** (1982) K21.

10. W. SCHAARWÄCHTER, *Phys. Status Solidi* **12** (1965) 865.
11. "Spravochnik Khimika" (Chemist's Handbook) 2nd Edition, Vol. 2 (Khimiya, Moscow, Leningrad, 1964).
12. "Poradnik Fizkochemiczny" (Physico-chemical Handbook) ("Naukowo-Techniczne" Press, Warsaw, 1974).
13. J. W. MULLIN, "Crystallization" 2nd Edition (Butterworths, London, 1972).
14. A. V. MISHCHENKO and L. N. RASHKOVICH, *Kristallogr.* **16** (1971) 1064.
15. K. H. HELLWEGE and A. M. HELLWEGE (EDS), "Numerical Data and Functional Relationships in Science and Technology" Group III, Vol. 11 (Springer-Verlag, Berlin, Heidelberg, New York, 1979).
16. J. J. GILMAN, *J. Appl. Phys.* **31** (1960) 2208.
17. V. D. KUZNETSOV, "Surface Energy of Solids" (HMSO, London, 1957).
18. J. D. DANA and C. S. HURLBUT Jr. "Dana's Manual of Mineralogy" (John Wiley and sons, New York, 1959).
19. C. H. GUIN, M. D. KATRICH, A. I. SAVINKOV and M. P. SHASKOLSKAYA, *Krist. Tech.* **15** (1980) 479.
20. A. R. PATEL and A. V. RAO, *J. Crystal Growth* **38** (1978) 288.
21. A. R. PATEL and S. K. ARORA, *Krist. Tech.* **13** (1978) 1445.
22. E. YU. GUTMANAS and E. M. NADGORNYI, *Fiz. Tverd. Tela* **11** (1969) 1179.
23. J. J. GILMAN, W. G. JOHNSTON and G. W. SEARS, *J. Appl. Phys.* **29** (1958) 747.
24. G. K. BARANOVA and E. M. NADGORNYI, *Kristallogr.* **17** (1972) 875.
25. V. HARI BABU and K. G. BANSIGIR, *J. Appl. Phys.* **38** (1967) 3399.
26. M. P. SHASKOLSKAYA, L. G. TSINZERLING and R. J. KULABUKHOVA, *Kristallogr.* **10** (1965) 121.
27. P. R. MORAN, *J. Appl. Phys.* **29** (1958) 1768.
28. E. YU. GUTMANAS and E. M. NADGORNYI, *Kristallogr.* **13** (1968) 114.
29. K. SANGWAL and A. A. URUSOVSKAYA, *J. Crystal Growth* **41** (1977) 216.
30. K. KISHAN RAO and D. B. SIRDESHMUKH, *ibid.* **44** (1978) 533.
31. E. B. TREIVUS, T. G. PETROV and J. E. KAMENTSEV, *Kristallogr.* **10** (1965) 380.
32. S. MURLIDHAR RAO and K. G. BANSIGIR, *Ind. J. Pure Appl. Phys.* **4** (1966) 363.
33. W. J. P. VAN ENCKEVORT and W. H. VAN DER LINDEN, *J. Crystal Growth* **46** (1979) 126.
34. K. SANGWAL and J. N. SUTARIA, *J. Mater. Sci.* **11** (1976) 2271.
35. A. R. PATEL and R. P. SINGH, *Japan. J. Appl. Phys.* **6** (1967) 938.
36. A. E. SMIRNOV and A. A. URUSOVSKAYA, *J. Mater. Sci.* **15** (1980) 1183.
37. A. R. PATEL and C. C. DESAI, *Z. Kristallogr.* **121** (1965) 54.
38. G. A. KEIG and R. L. KOBLE, *J. Appl. Phys.* **39** (1968) 6090.
39. W. J. P. VAN ENCKEVORT, R. JANSSEN VAN ROSMALLEN and W. H. VAN DER LINDEN, *J. Crystal Growth* **49** (1980) 502.
40. M. SZURGOT, J. KARNIEWICZ and W. KOLASIŃSKI, Extended Abstracts ICCG-6, edited by E. I. Givargizov (Moscow, 1980) Vol. IV, p. 141.
41. K. SANGWAL, M. SZURGOT, J. KARNIEWICZ and W. KOLASIŃSKI, to be published in *J. Crystal Growth* **58** (1982).
42. J. M. THOMAS, E. L. EVANS and T. A. CLARKE, *J. Chem. Soc.* A (1971) 2338.
43. A. R. PATEL and A. V. RAO, *J. Crystal Growth* **47** (1979) 213.
44. J. KARNIEWICZ, M. SZURGOT and B. WOJCIECHOWSKI, Extended Abstracts ICCG-6, edited by E. I. Givargizov (Moscow, 1980) Vol. IV, p. 135.
45. T. NAKAMURA and K. OHI, *J. Phys. Soc. Japan* **16** (1961) 209.
46. B. BORECKA, M. SZURGOT and B. WIKTOROWSKA, to be published.
47. A. R. PATEL and S. K. ARORA, *J. Mater. Sci.* **12** (1977) 2124.
48. O. P. BAHL and J. M. THOMAS, *ibid.* **2** (1967) 339.
49. T. NAKAMURA and K. OHI, *J. Phys. Soc. Japan* **15** (1960) 1348.
50. J. E. BRIGHT and M. J. RIDGE, *Phil. Mag.* **6** (1961) 441.
51. A. R. PATEL and K. S. RAJU, *Acta. Cryst.* **23** (1967) 217.
52. V. A. MELESHINA, T. F. CHERNYSHEVA and N. B. RUSSOVA, *Kristallogr.* **12** (1967) 371.
53. R. K. TAKU, Ph. D. THESIS, Sardar Patel University, India, (1971).
54. A. SAWADA and R. ABE, *Japan. J. Appl. Phys.* **6** (1962) 699.
55. J. M. THOMAS and J. O. WILLIAMS, *Trans. Faraday Soc.* **63** (1967) 1922.
56. K. SANGWAL and M. SZURGOT, *Cryst. Res. Technol.* **17** (1982) 49.
57. A. J. FORTY, *Phil. Mag.* **43** (1952) 72.
58. R. O. SHARKHATUNYAN, A. G. NALANDYAN and G. G. MURADYAN, *Kristallogr.* **21** (1976) 223.
59. A. KELLY and G. W. GROOVES, "Crystallography and Crystal Defects" (Longman, London, 1970).
60. K. SANGWAL, N. L. SIZOVA and A. A. URUSOVSKAYA, *Krist. Tech.* **12** (1977) 567.
61. V. N. ROZHANSKII, E. V. PARVOVA, V. M. STEPANOVA and A. A. PREDVODITELEV, *Kristallogr.* **6** (1961) 704.
62. A. A. URUSOVSKAYA, *ibid.* **8** (1963) 75.
63. Ya. GERASIMOV, V. DREVING, E. EREMIN, A. KISELEV, V. LEBEDEV, G. PANCHENKOV and A. SHLYGIN, "Physical Chemistry" Vol. 1 (Mir, Moscow, 1974).
64. K. SANGWAL, T. C. PATEL and M. D. KOTAK, *J. Mater. Sci.* **14** (1979) 1869.
65. K. SANGWAL and S. K. ARORA, *J. Phys. D: Appl. Phys.* **12** (1979) 645.

66. G. K. BARABOVA and E. M. NADGORNYI, *Kristallogr.* **20** (1975) 446.
67. N. F. KOSTIN, S. V. LUBENETS and K. S. ALEKSANDROV, *ibid.* **6** (1961) 737.
68. S. N. ANDREEV and V. G. KHALDIN, *Doklady Akad. Nauk SSSR* **134** (1962) 335.
69. S. N. ANDREEV and O. V. SAPOZHNIKOVA, *Zh. Neorg. Khimii* **13** (1968) 1548.
70. J. BJERUM, G. SCHWARZENBACH and L. G. SILLÉN, "Stability Constants" Part II (Chemical Society, London, 1958).
71. K. SANGWAL and T. C. PATEL, unpublished results (1980).
72. M. B. IVES and J. P. HIRTH, *J. Chem. Phys.* **33** (1960) 517.

Received 25 August
and accepted 15 December 1981